Research Article

Fatimah Mohammed Alzahrani, Abdelfattah Amari, Khadijah Mohammedsaleh Katubi*, Norah Salem Alsaiari*, Mohamed A. Tahoon

The synthesis of nanocellulose-based nanocomposites for the effective removal of hexavalent chromium ions from aqueous solution

https://doi.org/10.1515/chem-2022-0215
received April 15, 2022; accepted September 13, 2022

Abstract: The present study reports the synthesis of a polydopamine (PDA)/nanocellulose (NC) nanocomposite for the effective removal of chromium ions from water. PDA was used to modify NC surface producing a nanocomposite namely PDA/NC, by *in situ* polymerization of dopamine on the surface of NC. Thereafter, the as-synthesized nanocomposite was characterized using familiar techniques such as Fourier transform infrared, X-ray diffraction, X-ray photoelectron spectroscopy, ultraviolet-visible spectroscopy, and transmission electron microscopy. All results indicated the successful combination of PDA and NC in one nanocomposite. The PDA/NC nanocomposite was evaluated for the removal of hexavalent Cr(VI) ions from an aqueous solution. The adsorption conditions, such as pH, contact time, and initial Cr(VI) concentration, were optimized. Adsorption kinetic studies revealed that Cr(VI) removal on the surface of PDA/NC nanocomposite followed the pseudo-second-order kinetic model. Furthermore, isotherm studies revealed that Cr(VI) removal followed the Langmuir isotherm model with a maximum adsorption capacity (q_m) of 210 mg/g. The adsorption mechanism study indicated that the Cr(VI) removal was reached via complexation, adsorption, and chemical reduction. The reusability of a PDA/NC nanocomposite for the removal of Cr(VI) ions was studied up to five cycles with acceptable results. The high adsorption capacity and multiple removal mechanisms validated the effective applicability of PDA/NC nanocomposite as a useful adsorbent for the removal of Cr(VI) ions from aqueous solution.

Keywords: nanocomposites, nanocellulose, polydopamine, adsorption, water treatment, hexavalent chromium ions

*** Corresponding author: Khadijah Mohammedsaleh Katubi,** Department of Chemistry, College of Science, Princess Nourah bint Abdulrahman University, P.O. Box 84428, Riyadh 11671, Saudi Arabia, e-mail: kmkatubi@pnu.edu.sa
*** Corresponding author: Norah Salem Alsaiari,** Department of Chemistry, College of Science, Princess Nourah bint Abdulrahman University, P.O. Box 84428, Riyadh 11671, Saudi Arabia, e-mail: nsalsaiari@pnu.edu.sa
Fatimah Mohammed Alzahrani: Department of Chemistry, College of Science, Princess Nourah bint Abdulrahman University, P.O. Box 84428, Riyadh 11671, Saudi Arabia
Abdelfattah Amari: Department of Chemical Engineering, College of Engineering, King Khalid University, Abha 61411, Saudi Arabia; Department of Chemical Engineering & Processes, Research Laboratory of Processes, Energetics, Environment and Electrical Systems, National School of Engineers, Gabes University, Gabes 6072, Tunisia
Mohamed A. Tahoon: Department of Chemistry, College of Science, King Khalid University, P.O. Box 9004, Abha 61413, Saudi Arabia; Chemistry Department, Faculty of Science, Mansoura University, Mansoura 35516, Egypt

1 Introduction

Water pollution has posed a serious threat to human health and the environment [1–3]. The main pollutants of water are heavy metals, inorganic and organic chemicals, pesticides, and fertilizers. These pollutants mostly come from household wastes, agriculture, and chemical industries [4–6]. Among all pollutants, heavy metals are the most dangerous due to their high levels in water and inability to decompose [7,8]. Among all heavy metals, hexavalent chromium (Cr(VI)) is the most harmful to the environment [9,10]. Cr(VI) ions can cause genetic defects and cancer in living organisms and humans [11,12]. Therefore, industrial wastewater containing Cr(VI) ions must be treated before it is released into the environment. Several efforts have been made to remove Cr(VI) ions from aqueous solutions using many methods, including adsorption, ion exchange, photocatalysis, precipitation, and membrane separation [13–16]. Among all the methods used, adsorption is the most widely used due to its high efficiency, low cost, flexibility, and simple operation [17,18]. Several adsorbents have been investigated for the removal

of Cr(VI) ions, such as biomaterials, inorganic materials, and activated carbons [19–21]. However, due to its low capacity, its real application in the removal of Cr(VI) ions is limited. Therefore, there is a need to develop new adsorbents to remove Cr(VI) ions from aqueous solution with high efficiency.

Cellulose is a natural biopolymer originating from biomass plants, such as vines, straws, and trees, which make it so widely distributed and used. The mentioned sources can be used to synthesize cellulose using biological, chemical, and mechanical methods. Cellulose synthesized in the nanoscale range is known as nanocellulose (NC) [22]. NC has abundant hydroxyl groups, excellent mechanical properties, and a high specific surface area, which makes it an excellent adsorbent for removing pollutants from water. NC has been widely used as an adsorbent for removing toxic dyes and heavy metals from water [23–25]. But, the application of NC for the removal of heavy metals is limited due to its low adsorption capacity. This limitation can be overcome by modifying the surface of NC to increase its affinity and capacity toward the target adsorbate ions.

Polydopamine (PDA) is a promising material used in various applications, such as biomedical, environmental, and energy fields, due to its ability to bind metals and adhesion efficiency [26]. PDA is synthesized by the self-polymerization of dopamine, which has a high content of amine and catechol functional groups. These functional groups enable its interaction with inorganic and organic materials via non-covalent and covalent attachment. Recently, the adsorption capacities toward organic and metallic pollutants have been enhanced by modifying different adsorbents using PDA. For instance, chitosan hydrogel beads immobilized with silver nanoparticles were coated with PDA for antimicrobial activities and adsorption activity toward dyes and heavy metals [27]. Tungsten oxide@poly(vinylidene fluoride-*co*-hexafluoropropylene) electrospun nanofibers were coated with PDA to form a membrane with oil rejection ability and ampicillin degradation ability [28]. In addition, magnetic graphene oxide (GO/Fe_3O_4) nanoparticles were coated using PDA for the high removal efficiency of fluoroquinolone antibiotics, exceeding 95% [29]. In addition, MnO_2-loaded polyacrylonitrile was coated with PDA to form a composite of MnO_2/PDA/polyacrylonitrile fibers for the effective removal of lead (Pb^{2+}) ions [30]. Recently, PDA has been used to modify metal-organic framework (MOF) for the efficient removal of Pb^{2+} and Hg^{2+} heavy metals from water samples [31]. These studies show that the PDA is an excellent and promising modifier for various types of adsorbents, including magnetic nanoparticles, graphene, graphene oxides, chitosan, glass, and MOF. This is attributed to its unique chemical and physical properties, such as thermal stability, antioxidant properties, biocompatibility, binding ability, and adhesive properties.

In this context, the NC surface was functionalized using PDA to synthesize the nanocomposite (PDA/NC) that was investigated for the removal of Cr(VI) ions from the aqueous solution. The synthesized nanocomposite displayed high adsorption capacity, adsorption rate, and good reusability for the removal of Cr(VI) ions from water. The introduced adsorbent here proposes a hopeful candidate for efficient water treatment.

2 Materials and methods

2.1 Materials

Cotton pulp (99% cellulose content) was supplied by Alexandria Company for General Supplies, Egypt. Tris (hydroxymethyl)-aminomethane (Tris) was purchased from Shanghai Sinopharm Chemical Reagent. Dopamine hydrochloride and potassium dichromate ($K_2Cr_2O_7$) were purchased from Sigma-Aldrich. Sodium hydroxide (NaOH), sulfuric acid (H_2SO_4), hydrochloric acid (HCl), and aqueous ammonium (33%) were purchased from El-Gomhouria Co., Egypt. All chemicals were analytical grade and used without modification. Distilled water was used for the preparation of all solutions.

2.2 NC synthesis

NC was synthesized according to the literature [32] with certain modifications. A hydrolysis reaction of cotton pulp using H_2SO_4 was used for the synthesis of NC. Briefly, 2 g of cotton pulp was crushed and ground into fine portions, followed by treatment with 2% NaOH for 12 h at room temperature. Then, the solution was filtered and washed using distilled H_2O until it reached a neutral pH value. The resulting fine powder was dried and mixed with 16 mL of 65% H_2SO_4 for 40 min at 40°C with continuous stirring. The centrifugation at 4,000 rpm was used to obtain the product that was washed many times with distilled H_2O until it reached a neutral pH value. After that, ultra-sonication at 0°C for 30 min at 20 kHz was used to disperse the hydrolyzed cellulose in H_2O. Finally, the resultant NC suspension was freeze-dried to obtain the NC powder.

2.3 The synthesis of PDA particles

Typically, a mixed solvent of aqueous ammonia, ethanol, and deionized water was prepared with volumes of 1.12, 112, and 252 mL, respectively. Then, 28 mL of deionized water was used to dissolve 1.4 g of dopamine hydrochloride with continuous stirring for half hour. After that, the aqueous solution of dopamine was added to the previously prepared mixed solvent, and the reaction was left to undertake for 1 day in an open container with slow stirring. Finally, the solution was centrifuged for 15 min, and the synthesized PDA particles were collected and washed several times with deionized water.

2.4 The synthesis of PDA/NC nanocomposite

The synthesis of the PDA/NC nanocomposite was achieved through the *in situ* polymerization of dopamine monomer on the surface of NC. Typically, a homogenous suspension was obtained by mixing 1 g NC with 500 mL of distilled H_2O under the sonication process. After that, NC suspension was provided with 0.6 g of Tris, and the solution pH was kept at 8.5 using HCl and NaOH. At room temperature and with continuous stirring for 2 days in the air, the previous solution was provided with 1 g of dopamine to initiate the polymerization reaction. The solution slowly turned from pink to black color. Then, the centrifugation of the solution at 10,000 rpm was used to collect the product, and the PDA/NC solid was washed several times with distilled H_2O until the supernatant was clear. Finally, the solid PDA/NC nanocomposite was freeze-dried to be ready for characterization and application. Scheme 1 shows the synthesis of the PDA/NC nanocomposite for the removal of Cr(VI) ions.

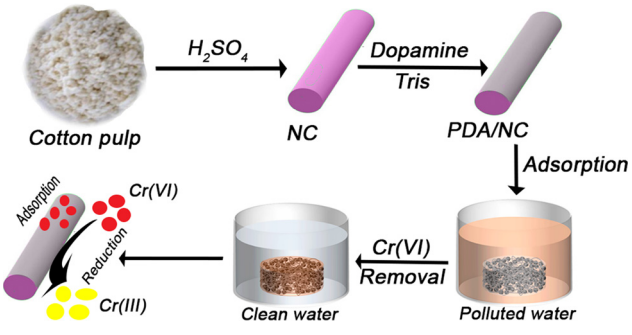

Scheme 1: Schematic illustration of the PDA/NC nanocomposite synthesis for the removal of Cr(VI) ions.

2.5 Equipment and apparatus

To confirm the combination of PDA and NC in the nanocomposite PDA/NC, various characterization techniques were used, including X-ray diffraction (XRD), Fourier transform infrared (FT-IR), X-ray photoelectron spectroscopy (XPS), ultraviolet (UV)-spectroscopy, and transmission electron microscopy (TEM). Functional groups and chemical structures of materials were investigated by the Tensor II FT-IR spectrometer (Bruker, Germany) over the range of 500–4,000 cm^{-1}. A D8 ADVANCE X-ray diffractometer from Bruker was used to obtain the XRD of materials to explore their crystalline structures. XRD was examined at a scanning rate of 5° min^{-1} in the range of 5–40°. The surface elements of the materials were examined using XPS (Thermo Fisher Scientific, USA). The material morphology was characterized using TEM (JEM-2100F; JEOL, Japan). N_2 sorption data were determined by the Brunauer–Emmett–Teller method (BET; Tristar II Plus; Micromeritics, USA) at 77 K. The thermal stability of the materials was determined using thermogravimetric analysis (TGA; PerkinElmer, USA). A pH meter (FE28; Mettler Toledo) was used to measure the pH value of the used solutions.

2.6 Cr(VI) removal experiments

A glass bottle was used to perform the adsorption experiments by stirring the mixture of a definite amount of PDA/NC nanocomposite with various concentrations of Cr(VI) ions solution at 25°C. The concentration of Cr(VI) ions was determined using a calibration curve by measuring the absorbance of the solution at 350 nm using a UV-visible (vis) spectrophotometer. The removal efficiency (%) and adsorption capacity (q_e) of PDA/NC nanocomposite toward Cr(VI) ions can be calculated according to equations (1) and (2), respectively.

$$\text{Removal efficiency}(\%) = ((C_0 - C_e)/C_0) \times 100, \quad (1)$$

$$\text{Adsorption capacity}(q_e) = ((C_0 - C_e)/m) \times V, \quad (2)$$

where C_0, C_e, m, and V denote Cr(VI) initial concentration, Cr(VI) concentration at equilibrium, the mass of PDA/NC nanocomposite in gram, and the volume of the solution in L, respectively. To study the pH effect on the Cr(VI) ions removal on the surface of synthesized materials, the adsorption experiments were performed at pH ranging from 2 to 11. The pH value was adjusted using 0.1 M of NaOH and H_2SO_4. The pH effect was studied using 100 mg/L of Cr(VI) solution, a volume of 10 mL, an adsorbent

dose of 10 mg, and stirring for 1 day at 25°C. The Cr(VI) content after each adsorption experiment was determined using a UV-vis spectrophotometer. To study the rate of Cr(VI) ions adsorption on the surface of synthesized materials, 12 mg of adsorbent was mixed with Cr(VI) ions at different initial concentrations ranging from 200 to 300 mg/L at a pH of 3, and the solution volume of 20 mL. At different times, the Cr(VI) ions content was determined using the UV-vis spectrophotometer to study the adsorption kinetics. To study the adsorption isotherm, different concentrations of Cr(VI) ions ranging from 30 to 600 mg/L were mixed with 6 mg of adsorbent at a pH of 3 for 1 day at 25°C using a volume solution of 10 mL. After each adsorption experiment, the solution was filtered and examined for the presence of Cr(VI) ions, and the adsorption capacity was determined to study the adsorption isotherm. The reusability of PDA/NC nanocomposite for the removal of Cr(VI) ions was studied up to five successive cycles of 0.5 M NaOH and 0.5 M sodium chloride for adsorbent regeneration after each cycle. During the reusability study, 10 mL of 20 mg/L Cr(VI) ions was mixed with 6 mg of adsorbent at 25°C for 12 h at a pH of 3. Then, the solution was filtered and examined for the presence of Cr(VI) ions, and the adsorbent was regenerated as described earlier. Then, the adsorbent was rinsed in distilled water and dried to be used in the next cycle.

3 Results and discussion

3.1 Characterization of PDA/NC nanocomposite

To study the crystallinity of the synthesized materials, XRD was performed, and the results are shown in Figure 1a. According to XRD results, the NC crystalline structure was found to be present in the PDA/NC nanocomposite, demonstrating that the addition of PDA did not affect the crystallinity of NC. According to the literature [33], the XRD of PDA/NC nanocomposite revealed the presence of cellulose I due to the appearance of diffraction planes (004), (200), (110), and (1–10) at 2θ = 34.6°, 22.8°, 16.8°, and 15.8°, respectively. Furthermore, the interaction between the PDA and the NC resulted in a reduction in peak intensity in the XRD of the PDA/NC nanocomposite.

To confirm the existence of functional groups, FT-IR spectra of PDA, NC, and PDA/NC were performed, and the results are shown in Figure 1b. According to the FT-IR results, the NC spectra showed the appearance of its specific bands corresponding to vibrations of water molecules, symmetric vibrations of C–H, and stretching vibrations of OH groups that appeared at 1,641, 2,904, and 3,418 cm^{-1}, respectively. While the spectra of the PDA/NC nanocomposite showed some modifications in the range of 1,600–1,200 cm^{-1} due to the addition of PDA to the NC. So, the presence of PDA was confirmed from FT-IR spectra by the appearance of bands at 1,285 and 1,509 cm^{-1} that correspond to the stretching vibration of C–O and the scissoring vibration of N–H, respectively [34].

Further characterization was performed using XPS spectra. The XPS full scan for NC and PDA/NC was performed as shown in Figure 1c. The XPS full scan of PDA/NC in comparison to NC showed the appearance of an additional peak at 403 eV related to N1s and confirmed the existence of PDA in the nanocomposite as reported in the literature [35]. In addition, the XPS high resolution C1s spectra were obtained for NC and PDA/NC nanocomposite, as shown in Figure 1d and e, respectively. The high resolution of C1s spectra of NC showed the appearance of four fractions at 289.1, 288.07, 286.6, and 285.1 eV that correspond to O–C═O, O–C–O/C═O, C–O, and C–C/C–H, respectively, as reported in the literature [36]. The high resolution of the C1s spectra of PDA/NC showed the appearance of the same fractions as well as the appearance of an additional fraction at 286.3 eV that corresponds to C–N, indicating a well combined PDA and NC in one composite.

Furthermore, the UV-vis spectra of both NC and PDA/NC were performed, and the results are shown in Figure 1f. The comparison of the two peaks showed the appearance of an additional peak at 280.0 nm by the addition of PDA to the surface of NC. This additional peak corresponds to the PDA parts and results from the π–π^* transition as reported in a previous study [37]. All the above results indicate the well-functionalization of the NC surface with PDA.

To study morphology and the size of synthesized materials, the TEM images of NC and PDA/NC nanocomposite are shown in Figure 2a and b, respectively. According to Figure 2a, the acid hydrolysis of cotton pulp led to the successful synthesis of NC with a diameter of 13 nm. While the TEM image of the PDA/NC nanocomposite showed an increase in diameter after the addition of PDA to 15 nm. Figure 2b shows the successful functionalization of the NC surface with PDA. This functionalization was achieved as described in the literature [38] by the reaction of hydroxyl groups in NC with catechol groups in the PDA followed by the dehydration process to produce a charge-transfer complex. This functionalization is responsible for the diameter increase as well as the morphological change.

Furthermore, TGA was used to determine the thermal stability of the synthesized nanomaterials, and the results

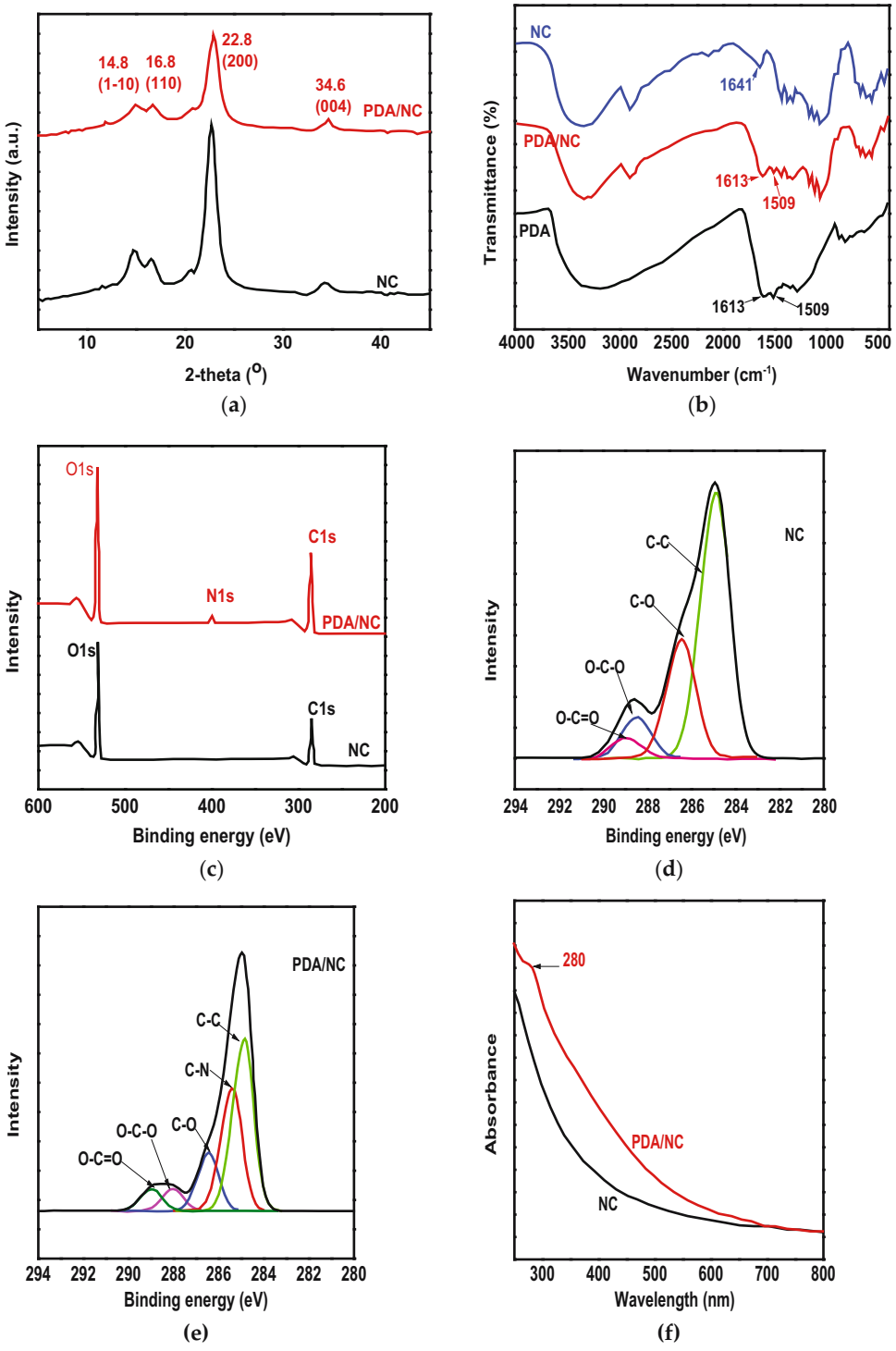

Figure 1: XRD (a), FT-IR (b), full-range XPS spectra (c), for NC (d), for PDA/NC (e), and UV-vis spectra (f) of NC and PDA/NC nanocomposite.

are shown in Figure 3a. According to TGA results, at 100°C, the synthesized NC showed a weight loss of 3% that resulted from the evaporation of adsorbed H_2O. At 280°C, NC was degraded and, subsequently, it showed a weight loss of 71%. While at 390°C, the NC residuals were decomposed into carbon dioxide and water and showed a weight loss of 24% [39]. For PDA, the heating under a nitrogen atmosphere to 800°C showed a residual weight of 56% in a multistep loss, indicating the heterogeneous construction of PDA.

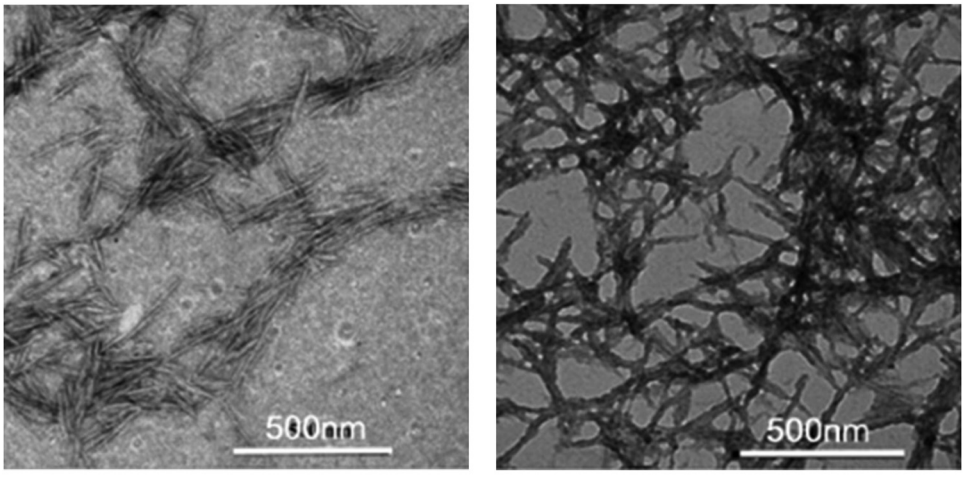

Figure 2: TEM image of (a) NC and (b) PDA/NC nanocomposite.

For PDA/NC nanocomposite, at 100°C, the adsorbed H_2O molecules evaporated, causing a weight loss of 7%. At 280°C, the degradation of PDA and NC caused another weight loss of 31%. The weight loss of the PDA/NC nanocomposite reached 66% at a temperature of 800°C. The TGA results indicated that the PDA successfully functionalized the NC and enhanced its thermal stability. To study the effect of PDA on the improvement of NC surface area, the BET surface area was determined for NC and PDA/NC nanocomposite, and the results are shown in Figure 3b. The determined BET surface was found to be 0.75 and 107.5 m^2/g for NC and PDA/NC, respectively. This enhanced surface area resulted from the addition of PDA to NC that improved the stability of the nanocomposite as well as the adsorption active site on the surface of the nanosorbent. This enhanced area will be very helpful to the uptake of more Cr(VI) ions from the aqueous solution during the adsorption process. All the above characterization techniques indicated the successful integration of PDA on the surface of NC to produce a PDA/NC nanocomposite.

3.2 Optimization of the adsorption conditions

To optimize the adsorption process of Cr(VI) ions on the surface of PDA/NC nanocomposite, the effect of different conditions like pH, initial Cr(VI) ions concentration, and

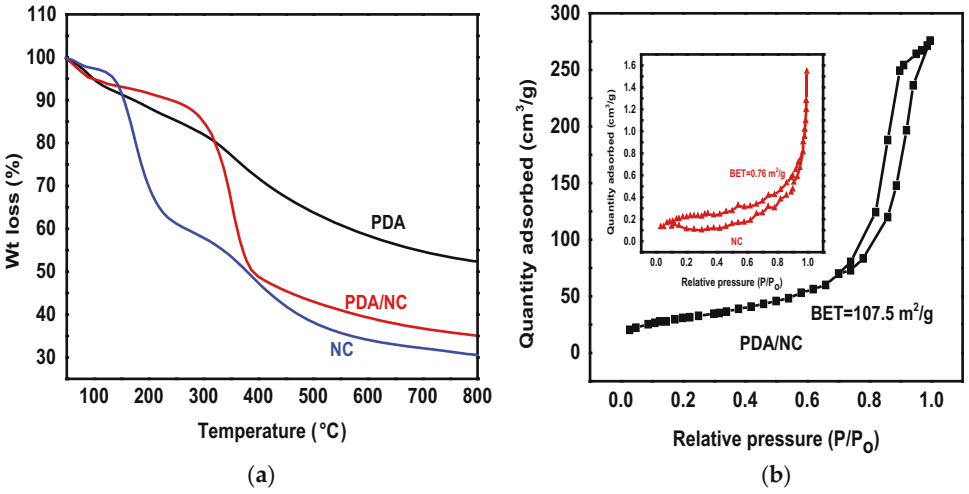

Figure 3: TGA (a) and nitrogen adsorption–desorption isotherm (b) of synthesized NC, PDA, and PDA/NC nanocomposite.

contact time must be studied. Subsequently, the effect of the aforementioned conditions was studied as shown in Figure 4. The effect of initial Cr(VI) ions concentration was studied in the concentration range of 30–130 mg/L at fixed pH of 3 and room temperature, and the results are shown in Figure 4a. According to Figure 4a, the highest removal efficiency of Cr(VI) ions was reached at an initial concentration of 50 mg/L and found to equal 100%. When the initial concentration was increased from 50 to 65 mg/L, the removal efficiency decreased to 87%, and the continuous increase in initial concentration led to a gradual decrease in removal efficiency until it reached the lowest value (55%) at 130 mg/L. This behavior can be interpreted on the basis that the PDA/NC adsorbent has a fixed number of adsorption sites at a fixed dose of adsorbent. So, the low initial concentration of Cr(VI) ions can be adsorbed over sufficient numbers of active sites, and hence, the removal efficiency was increased. But, the increased initial concentration of Cr(VI) ions led to the uptake of ions corresponding to the fixed number of sites, and hence, the removal efficiency was decreased. This behavior of removal efficiency with the initial concentration of Cr(VI) ions was observed in several reported studies [40,41].

As the adsorbent–Cr(VI) interaction greatly depends on the pH value, the solution pH is an essential parameter affecting the Cr(VI) removal [42]. According to pH value, Cr(VI) species are present. At pH < 1, H_2CrO_4 is the main form of chromium ions. At a pH range of 2–6, $Cr_2O_7^{2-}$ and $HCrO_4^-$ are the main forms of chromium ions. At pH > 6, CrO_4^{2-} is the main form of chromium ions. This dependence of chromium existence on the pH value was explained in our previous study [43]. The effect of pH on the adsorption of Cr(VI) ions over PDA/NC nanocomposite was studied in the range of 3–11, and the results are shown in Figure 4b. According to Figure 4b, the increased pH value led to a

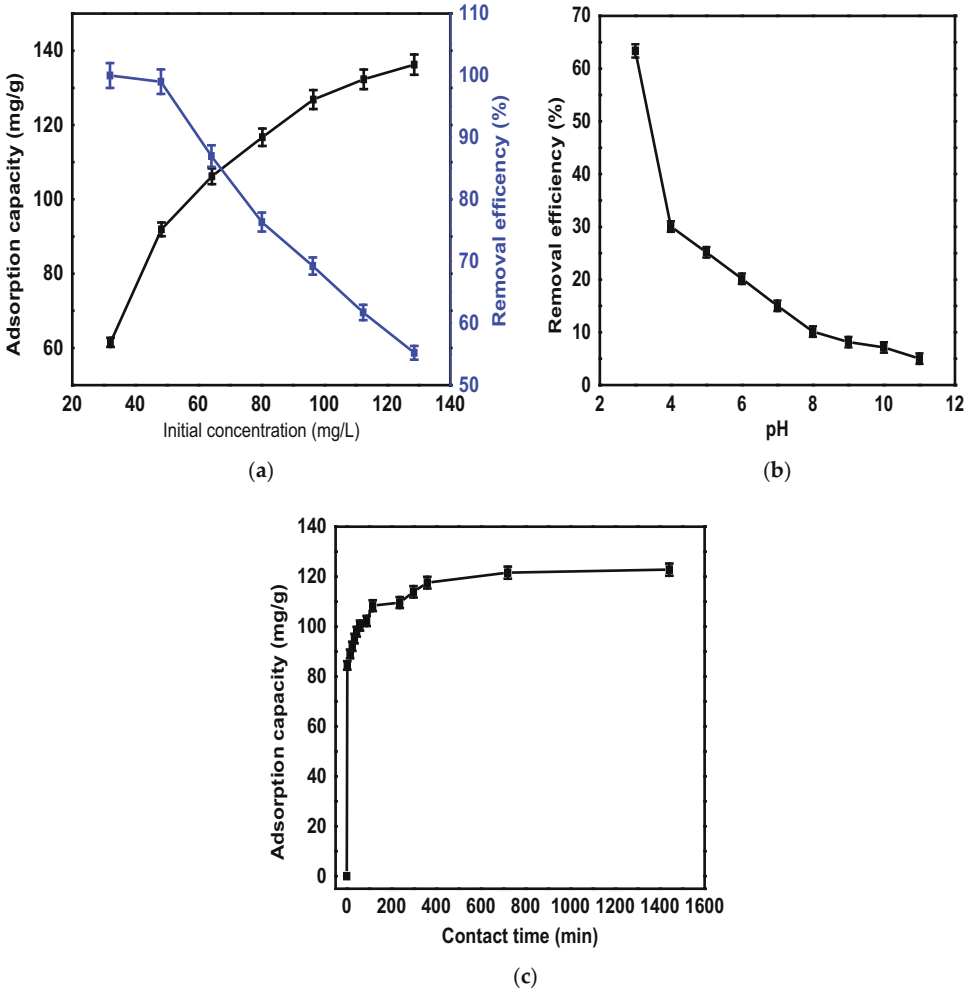

Figure 4: The effect of pH (a), initial concentration (b), and contact time (c) on the removal of Cr(VI) ions over the surface of PDA/NC nanocomposite.

decreased removal efficiency of Cr(VI) ions. The highest removal efficiency was reached at a pH value of 3. This behavior can be attributed to the strong interaction between the protonated surface of the PDA/NC nanocomposite at a low pH value and the anion species of chromium ions [44]. The excess H^+ ions at low pH values cause protonation of functional groups on the surface of the adsorbent to form a positively charged adsorbent that can capture the negatively charged chromium ions through electrostatic interaction, and hence, the removal efficiency was increased. So, the optimum pH value for the removal of Cr(VI) ions on PDA/NC nanocomposite is 3. While at a higher pH value, the excess OH^- ions were repulsed by negatively charged chromium ions and caused a decrease in the removal efficiency. This behavior of pH effect on Cr(VI) removal was observed in many reported studies [45,46].

To optimize the contact time for the removal of Cr(VI) ions on the surface of PDA/NC nanocomposite, the adsorption experiment was employed at different time intervals ranging from 0 to 1,600 min. Figure 4c displays the removal capacity of PDA/NC nanocomposite toward Cr(VI) ions at different contact times. According to Figure 4c, there are two stages of adsorption until equilibrium is reached: the slow stage and the rapid stage. The initial rapid phase showed an improved adsorption capacity of PDA/NC nanocomposite toward Cr(VI) ions. Subsequently, the optimum contact time for the adsorption of Cr(VI) ions is 6 h. Further increases in contact time over 6 h led to the appearance of a second slow phase. This phase showed a negligible effect of contact time on the adsorption of Cr(VI) ions on the surface of the PDA/NC nanocomposite. The initial stage showed a rapid and enhanced adsorption capacity toward Cr(VI) ions due to the availability of various active sites during this stage [47]. While at the second stage, the sites become saturated and the ions compete with each other for active sites [47], and the contact time has no significant effect here.

3.3 Adsorption kinetics

The controlling mechanism of Cr(VI) uptake by PDA/NC can be explained using the kinetic study. To explain the adsorption process of Cr(VI) ions on the surface of PDA/NC nanocomposite, the kinetic experimental data were fitted using two kinetic models, namely pseudo-first-order and pseudo-second-order models [48]. The pseudo-first-order and pseudo-second-order models can be expressed according to equations (3) and (4), respectively.

$$\ln\ q_e - q_t = \ln\ q_e - k_1 t, \tag{3}$$

$$\frac{t}{q_t} = \left(\frac{1}{k_2 {q_e}^2}\right) + t/q_e, \tag{4}$$

where q_t, q_e, k_1, and k_2 denote the adsorption capacity at time t (min), the adsorption capacity at equilibrium, the pseudo-first-order kinetic adsorption rate constant, and the pseudo-second-order kinetic adsorption rate constant, respectively. Figure 5 shows the fitting of experimental data to pseudo-first-order and pseudo-second-order kinetic models, and their calculated parameters are tabulated in Table 1.

The experimental value of q_e was closer to the calculated value from the pseudo-second-order model than the

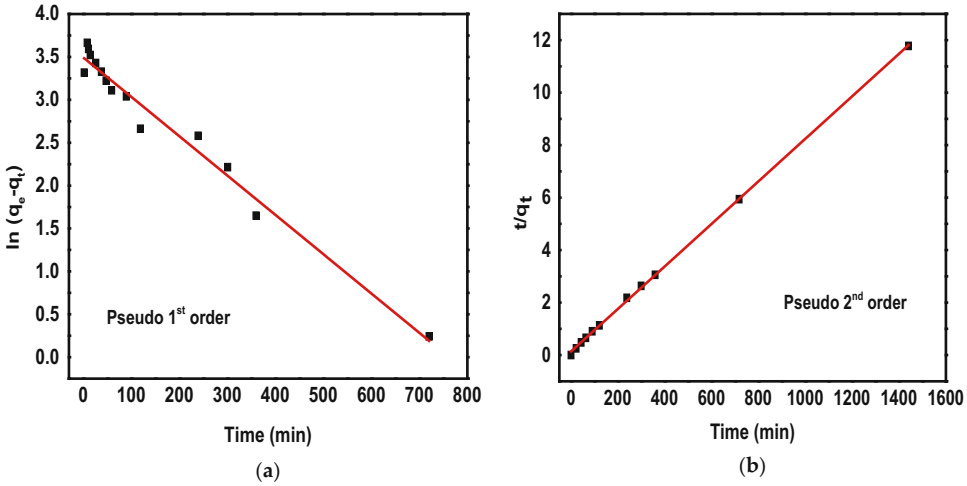

Figure 5: The fitting of experimental data to pseudo-first-order model (a) and pseudo-second-order model (b) for the adsorption of Cr(VI) ions on the surface of PDA/NC nanocomposite.

Table 1: The kinetic parameters of pseudo-first-order and pseudo-second-order models for the removal of Cr(VI) on the surface of PDA/NC nanocomposite

Pseudo first order					Pseudo second order	
q_e (exp) (mg/g)	q_e (cal) (mg/g)	K_1	R^2	q_e (cal) (mg/g)	K_2	R^2
123	33.42	0.0048	0.960	123.48	0.00067	0.9991

pseudo-first-order model. Also, the R^2 values as presented in Table 1 indicated that the removal of Cr(VI) ions on the surface of PDA/NC nanocomposite best fits the pseudo-second-order model than the pseudo-first-order model. These results indicate that the adsorption of Cr(VI) ions on the surface of the PDA/NC nanocomposite was achieved through a chemical adsorption process [49,50]. The chemical adsorption behavior indicates that the interaction between the functional groups on the surface of PDA/NC nanocomposite and the Cr(VI) ions occurred via a very strong complexation reaction.

3.4 Adsorption isotherm

To describe the adsorption process of Cr(VI) ions on the surface of PDA/NC nanocomposite, Langmuir and Freundlich isotherm models were used. The Langmuir and Freundlich isotherm models are represented according to equations (5) and (6), respectively.

$$1/q_e = (1/q_m K_L)C_e + 1/q_m, \quad (5)$$

$$\ln\ q_e = \ln\ K_F + \frac{1}{n}\ln\ C_e, \quad (6)$$

where q_m, K_L, K_F, and $1/n$ represent the maximum adsorption capacity (mg/g), Langmuir constant, Freundlich constant, and adsorption intensity factor, respectively.

Langmuir isotherm model suggests the monolayer homogenous adsorption of the adsorbate ions over the energetically similar active sites [51]. While the Freundlich isotherm model suggests the multilayer heterogeneous adsorption of the adsorbate ions [51]. The fitting of experimental data to Langmuir and Freundlich isotherm models is presented in Figure 6, and their calculated parameters were introduced in Table 2. The correlation coefficient (R^2) determines the suitability of the isotherm model to describe the adsorption process. According to the linearization curves of Langmuir and Freundlich's isotherms shown in Figure 6 and the R^2 values in Table 2, the adsorption of Cr(VI) onto the surface of PDA/NC nanocomposite follows the Langmuir isotherm model. The results indicated that the uptake of Cr(VI) ions on the PDA/NC nanocomposite surface occurred via monolayer adsorption. In addition, the maximum adsorption capacity (q_m) of PDA/NC nanocomposite is 210 mg/g, which is considered to be very high when compared to other adsorbents used for the removal of Cr(VI) ions. This enhanced adsorption capacity could be attributed to a large number of

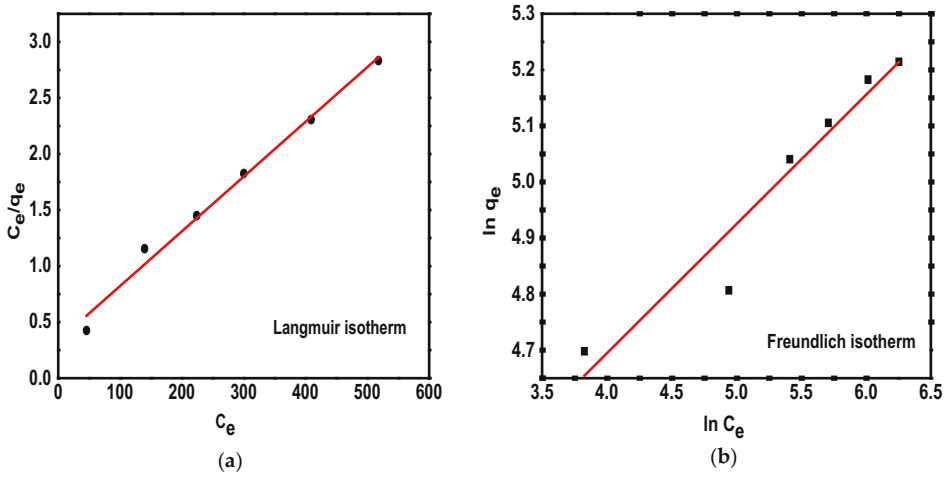

Figure 6: The fitting of experimental data to Langmuir isotherm (a) and Freundlich isotherm (b) for the adsorption of Cr(VI) ions on the surface of PDA/NC nanocomposite.

Table 2: The parameters of Freundlich and Langmuir isotherm models for the removal of Cr(VI) on the surface of PDA/NC nanocomposite

Langmuir			Freundlich		
q_m (mg/g)	K_L	R^2	K_F	n	R^2
210	0.0148	0.988	43.30	4.35	0.911

functional groups on the surface of the adsorbent due to the modification using PDA.

3.5 Adsorption mechanism

The study of the removal mechanism gives a deep insight into the efficiency and action of the adsorbent during the treatment. To determine the mechanism of Cr(VI) removal on the surface of PDA/NC nanocomposite, XPS high-resolution Cr 2p spectra were performed on PDA/NC nanocomposite after the removal of Cr(VI) ions on its surface. Figure 7 shows the XPS Cr 2p spectra of the PDA/NC nanocomposite. According to Figure 7, there are two different species of chromium ions present (Cr(III) and Cr(VI)). The integration area from the obtained spectra clearly shows the existence of these two ions on the adsorbent after water treatment. These results indicated that the Cr(VI) ions were removed from the surface of the studied adsorbent through two different mechanisms. In the first way, the catechol functional groups of PDA on the surface of NC reduced Cr(VI) to Cr(III) and itself was oxidized to COOH– groups. Moreover, the electrons for the reduction of Cr(VI) are moved from nitrogen functional groups (catechol) of PDA as electron-donating groups, causing the oxidation of catechol groups to COOH– groups. The formed Cr(III) ions have vacant shell orbital that can receive lone-pair electrons from amine groups of PDA, causing the creation of a chelated complex. In a second way, the functional groups of PDA (amine and catechol) strongly chelate or electrostatically attract the Cr(VI) ions on the surface of the adsorbent. Based on the above analysis, Cr(VI) removal on the surface of PDA/NC nanocomposite was attributed to complexation, adsorption, and chemical reduction. These multiple removal mechanisms validated the effective applicability of PDA/NC nanocomposite as a perfect adsorbent for the removal of Cr(VI) ions from an aqueous solution.

3.6 Regeneration and reusability study

The reusability of any adsorbent is an important factor for use in large-scale water treatment, as it reduces the overall cost of treatment [52–56]. The reusability of PDA/NC nanocomposite was studied for the removal of Cr(VI) ions up to five successive cycles. Figure 8 shows the reusability study of PDA/NC nanocomposite as an adsorbent for Cr(VI) ions. Each cycle consists of an adsorption part followed by a desorption. The nanocomposite was used for the adsorption of Cr(VI) ions followed by the collection of nanocomposite and washing by NaOH and NaCl to desorb attached Cr(VI) ions and regenerate the adsorption sites. After each cycle, the solution was examined for the existence of Cr(VI) ions. According to Figure 8, the highest removal efficiency was achieved for the first cycle due to the presence of fresh unused active sites.

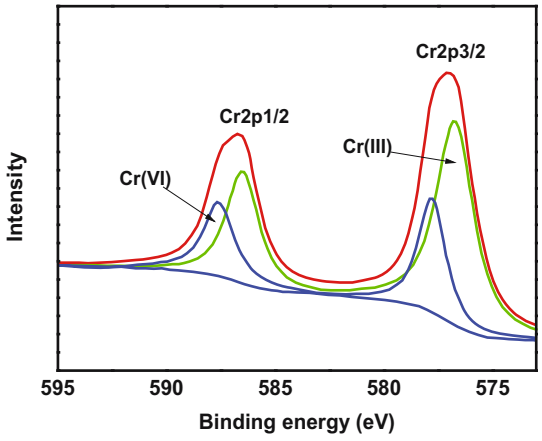

Figure 7: XPS high-resolution Cr 2p spectra of PDA/NC nanocomposite after the removal of Cr(VI) ions.

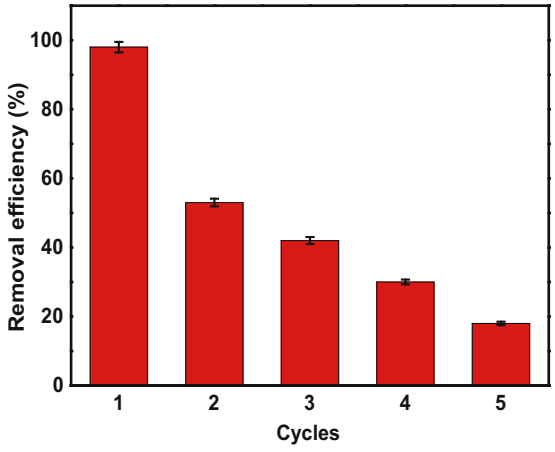

Figure 8: Reusability of PDA/NC nanocomposite for the removal of Cr(VI) ions up to five cycles.

Table 3: The comparison between different adsorbents for the removal of Cr(VI) ions

Adsorbent	Adsorption capacity (mg/g)	References
PDA/NC	210	This study
NiCo-LDH	100	[58]
Ppy/Fe_3O_4 magnetic nanocomposite	169.4	[59]
Fe_2O_3@SiO_2	153	[60]
Magnetic SiO_2@$CoFe_2O_4$ nanoparticles	136.4	[61]
Bentonite clay@$MnFe_2O_4$ composite	178.57	[47]
Sodium alginate-polyaniline	73.34	[62]
Stacked CS	131.58	[63]
Polyacrylonitrile/NH_2	156	[64]
Fe_3O_4@SBA-15-PDA/HBP-NH_2	66.5	[65]
Mn-incorporated ferrihydrite	48.5	[66]
ppy@magnetic chitosan	105.0	[67]

After that, the removal efficiency decreased from one cycle to another until it reached the minimum efficiency in the fifth cycle. The nanocomposite lost 92% of its efficiency in the last cycle. This means that most of the adsorption sites on the surface of PDA/NC nanocomposites cannot be regenerated, and subsequently, poor reusability results. This can be attributed to the mechanism of removal as the sites removed Cr(VI) by adsorption can be regenerated, while the sites removed Cr(VI) by reduction (which involved the oxidation of catechol groups to carboxylic groups) cannot be regenerated as reported in the literature [57].

3.7 Comparative study

The PDA/NC nanocomposite synthesized in the present study showed a high adsorption capacity. This adsorption capacity was compared with the capacities of previously reported adsorbents for Cr(VI) removal as presented in Table 3. According to the comparison in Table 3, the PDA/NC nanocomposite showed excellent adsorption capacity compared to other reported adsorbents.

4 Conclusion

In this work, PDA-functionalized NC was fabricated using *in situ* polymerization of dopamine on the surface of NC. The as-synthesized PDA/NC nanocomposite was well characterized, indicating the successful fabrication of the hybrid nanocomposite. The PDA/NC nanocomposite showed a higher BET surface area than NC that attributed to the addition of PDA on the surface of NC. Moreover, the PDA/NC nanocomposite showed enhanced thermal stability compared to its parts. The synthesized adsorbent showed good adsorption toward Cr(VI) ions from an aqueous solution at optimum conditions of pH, contact time, and initial concentration. The study of adsorption kinetics indicated that the removal of Cr(VI) follows the pseudo-second-order kinetic model. The study of adsorption isotherm indicated the monolayer removal of Cr(VI) on the energetically identical active sites. In addition, the maximum adsorption capacity (q_m) was found to be 210 mg/g. The removal mechanism was studied, indicating the elimination of Cr(VI) ions from aqueous solution in three ways, including adsorption, complexation, and chemical reduction. The reusability of the synthesized nanocomposite was studied for up to five cycles, with poor results attributed to the mechanism of removal and damaged active sites. According to the results, the PDA/NC nanocomposite is a promising candidate for the removal of Cr(VI) ions from water.

Acknowledgment: The authors extend their appreciation to the Deanship of Scientific Research at King Khalid University for funding this work through the research groups program under Grant No. GRP/88/43. Furthermore, this research was funded by Princess Nourah bint Abdulrahman University Researchers Supporting Project No. PNURSP2022R42, Princess Nourah bint Abdulrahman University, Riyadh, Saudi Arabia.

Funding information: This research was funded by the Deanship of Scientific Research at King Khalid University under grant number GRP/88/43. Additionally, this research was funded by Princess Nourah bint Abdulrahman University Researchers Supporting Project number (PNURSP2022R42), Princess Nourah bint Abdulrahman University, Riyadh, Saudi Arabia.

Author contributions: All authors contributed equally to this study.

Conflict of interest: The authors declare that they have no conflicts of interest.

Ethical approval: The conducted research is not related to either human or animal use.

Data availability statement: The research data used to support the findings of this study are included within the article.

References

[1] Siddeeg SM, Amari A, Tahoon MA, Alsaiari NS, Rebah FB. Removal of meloxicam, piroxicam and Cd^{+2} by Fe_3O_4/SiO_2/glycidyl methacrylate-S-SH nanocomposite loaded with laccase. Alex Eng J. 2020;59(2):905–14. doi: 10.1016/j.aej.2020.03.018.

[2] Tahoon MA, Siddeeg SM, Salem Alsaiari N, Mnif W, Ben Rebah F. Effective heavy metals removal from water using nanomaterials: A review. Processes. 2020;8(6):645. doi: 10.3390/pr8060645.

[3] Alzahrani FM, Alsaiari NS, Katubi KM, Amari A, Ben Rebah F, Tahoon MA. Synthesis of polymer-based magnetic nanocomposite for multi-pollutants removal from water. Polymers. 2021;13(11):1742. doi: 10.3390/polym13111742.

[4] Singh C, Tiwari S, Singh JS. Biochar: A sustainable tool in soil pollutant bioremediation. Bioremediation of industrial waste for environmental safety. Singapore: Springer; 2020. p. 475–94.

[5] El-Gaayda J, Titchou FE, Oukhrib R, Yap P-S, Liu T, Hamdani M, et al. Natural flocculants for the treatment of wastewaters containing dyes or heavy metals: A state-of-the-art review. J Environ Chem Eng. 2021;9:106060. doi: 10.1016/j.jece.2021.106060.

[6] Bankole MT, Abdulkareem AS, Mohammed IA, Ochigbo SS, Tijani JO, Abubakre OK, et al. Selected heavy metals removal from electroplating wastewater by purified and polyhydroxylbutyrate functionalized carbon nanotubes adsorbents. Sci Rep. 2019;9(1):1–19. doi: 10.1038/s41598-018-37899-4.

[7] Su Y-Q, Zhao Y-J, Wu N, Chen Y-E, Zhang W-J, Qiao D-R, et al. Chromium removal from solution by five photosynthetic bacteria isolates. Appl Microbiol Biotechnol. 2018;102(4):1983–95. doi: 10.1007/s00253-017-8690-x.

[8] Venkateswarlu S, Panda A, Kim E, Yoon M. Biopolymer-coated magnetite nanoparticles and metal–organic framework ternary composites for cooperative Pb (II) adsorption. ACS Appl Nano Mater. 2018;1(8):4198–210. doi: 10.1021/acsanm.8b00957.

[9] Islam MA, Angove MJ, Morton DW, Pramanik BK, Awual MR. A mechanistic approach of chromium (VI) adsorption onto manganese oxides and boehmite. J Environ Chem Eng. 2020;8(2):103515. doi: 10.1016/j.jece.2019.103515.

[10] Liu W, Yang L, Xu S, Chen Y, Liu B, Li Z, et al. Efficient removal of hexavalent chromium from water by an adsorption–reduction mechanism with sandwiched nanocomposites. RSC Adv. 2018;8(27):15087–93. doi: 10.1039/C8RA01805G.

[11] Fei X, Ling Y, Shan Q, Hei D, Jia W. Catalytic effect of a semiconductor on the removal of hexavalent chromium from aqueous solution by γ-ray irradiation. Water Air Soil Pollut. 2017;228(9):1–6. doi: 10.1007/s11270-017-3535-x.

[12] Hmamou M, Sbihi K, Ammary B, Bellaouchou A. Study of chromium adsorption by iron hydroxide. Mater Today Proc. 2020;24:52–9. doi: 10.1016/j.matpr.2019.07.528.

[13] Xiao X, Deng Y, Xue J, Gao Y. Adsorption of chromium by functionalized metal organic frameworks from aqueous solution. Environ Technol. 2021;42(12):1930–42. doi: 10.1080/09593330.2019.1683618.

[14] Peng H, Guo J. Removal of chromium from wastewater by membrane filtration, chemical precipitation, ion exchange, adsorption electrocoagulation, electrochemical reduction, electrodialysis, electrodeionization, photocatalysis and nanotechnology: A review. Environ Chem Lett. 2020;18:2055–68. doi: 10.1007/s10311-020-01058-x.

[15] Zhao Z, An H, Lin J, Feng M, Murugadoss V, Ding T, et al. Progress on the photocatalytic reduction removal of chromium contamination. Chem Rec. 2019;19(5):873–82. doi: 10.1002/tcr.201800153.

[16] Dognani G, Hadi P, Ma H, Cabrera FC, Job AE, Agostini D.L.S, Hsiao BS., Effective chromium removal from water by polyaniline-coated electrospun adsorbent membrane. Chem Eng J. 2019;372:341–51. doi: 10.1016/j.cej.2019.04.154.

[17] Amari A, Elboughdiri N, Ghernaout D, Lajimi RH, Alshahrani AM, Tahoon MA, et al. Multifunctional crosslinked chitosan/nitrogen-doped graphene quantum dot for wastewater treatment. Ain Shams Eng J. 2021;12:4007–14. doi: 10.1016/j.asej.2021.02.024.

[18] Dai Y, Sun Q, Wang W, Lu L, Liu M, Li J, et al. Utilizations of agricultural waste as adsorbent for the removal of contaminants: A review. Chemosphere. 2018;211:235–53. doi: 10.1016/j.chemosphere.2018.06.179.

[19] Fotsing PN, Woumfo ED, Mezghich S, Mignot M, Mofaddel N, Le Derf F, et al. Surface modification of biomaterials based on cocoa shell with improved nitrate and Cr (vi) removal. RSC Adv. 2020;10(34):20009–19. doi: 10.1039/D0RA03027A.

[20] Gallo-Cordova A, Morales MDP, Mazarío E. Effect of the surface charge on the adsorption capacity of chromium (VI) of iron oxide magnetic nanoparticles prepared by microwave-assisted synthesis. Water. 2019;11(11):2372. doi: 10.3390/w11112372.

[21] Tu B, Wen R, Wang K, Cheng Y, Deng Y, Cao W, et al. Efficient removal of aqueous hexavalent chromium by activated carbon derived from Bermuda grass. J Colloid Interface Sci. 2020;560:649–58. doi: 10.1016/j.jcis.2019.10.103.

[22] Wei J, Yang Z, Sun Y, Wang C, Fan J, Kang G, et al. Nanocellulose-based magnetic hybrid aerogel for adsorption of heavy metal ions from water. J Mater Sci. 2019;54(8):6709–18. doi: 10.1007/s10853-019-03322-0.

[23] Qiao A, Cui M, Huang R, Ding G, Qi W, He Z, et al. Advances in nanocellulose-based materials as adsorbents of heavy metals and dyes. Carbohydr Polym. 2021;272:118471. doi: 10.1016/j.carbpol.2021.118471.

[24] Tshikovhi A, Mishra SB, Mishra AK. Nanocellulose-based composites for the removal of contaminants from wastewater.

Int J Biol Macromol. 2020;152:616–32. doi: 10.1016/j.ijbiomac.2020.02.221.
[25] Faiz Norrrahim MN, Mohd Kasim NA, Knight VF, Mohamad Misenan MS, Janudin N, Ahmad Shah NA, et al. Nanocellulose: A bioadsorbent for chemical contaminant remediation. RSC Adv. 2021;11(13):7347–68. doi: 10.1039/D0RA08005E.
[26] Liu Y, Ai K, Lu L. Polydopamine and its derivative materials: Synthesis and promising applications in energy, environmental, and biomedical fields. Chem Rev. 2014;114(9):5057–115. doi: 10.1021/cr400407a.
[27] Wang T, Kuttappan D, Amalaradjou MA, Luo Y, Luo Y. Polydopamine-coated chitosan hydrogel beads for synthesis and immobilization of silver nanoparticles to simultaneously enhance antimicrobial activity and adsorption kinetics. Adv Compos Hybrid Mater. 2021;4(3):696–706. doi: 10.1007/s42114-021-00305-1.
[28] Mavukkandy MO, Ibrahim Y, Almarzooqi F, Naddeo V, Karanikolos GN, Alhseinat E, et al. Synthesis of polydopamine coated tungsten oxide@poly (vinylidene fluoride-*co*-hexafluoropropylene) electrospun nanofibers as multifunctional membranes for water applications. Chem Eng J. 2022;427:131021. doi: 10.1016/j.cej.2021.131021.
[29] Tan F, Liu M, Ren S. Preparation of polydopamine-coated graphene oxide/Fe_3O_4 imprinted nanoparticles for selective removal of fluoroquinolone antibiotics in water. Sci Rep. 2017;7(1):1–9. doi: 10.1038/s41598-017-06303-y.
[30] Li Y, Zhao R, Chao S, Sun B, Wang C, Li X. Polydopamine coating assisted synthesis of MnO_2 loaded inorganic/organic composite electrospun fiber adsorbent for efficient removal of Pb^{2+} from water. Chem Eng J. 2018;344:277–89. doi: 10.1016/j.cej.2018.03.044.
[31] Sun DT, Peng L, Reeder WS, Moosavi SM, Tiana D, Britt DK, et al. Rapid, selective heavy metal removal from water by a metal–organic framework/polydopamine composite. ACS Cent Sci. 2018;4(3):349–56. doi: 10.1021/acscentsci.7b00605.
[32] Neto WPF, Silvério HA, Dantas NO, Pasquini D. Extraction and characterization of cellulose nanocrystals from agro-industrial residue–Soy hulls. Ind Crop Prod. 2013;42:480–8. doi: 10.1016/j.indcrop.2012.06.041.
[33] French AD. Idealized powder diffraction patterns for cellulose polymorphs. Cellulose. 2014;21(2):885–96. doi: 10.1007/s10570-013-0030-4.
[34] Liu W, Li Y, Meng X, Liu G, Hu S, Pan F, et al. Embedding dopamine nanoaggregates into a poly (dimethylsiloxane) membrane to confer controlled interactions and free volume for enhanced separation performance. J Mater Chem A. 2013;1(11):3713–23. doi: 10.1039/C3TA00766A.
[35] Yu Y, Shapter JG, Popelka-Filcoff R, Bennett JW, Ellis AV. Copper removal using bio-inspired polydopamine coated natural zeolites. J Hazard Mater. 2014;273:174–82. doi: 10.1016/j.jhazmat.2014.03.048.
[36] Chao C, Liu J, Wang J, Zhang Y, Zhang B, Zhang Y, et al. Surface modification of halloysite nanotubes with dopamine for enzyme immobilization. ACS Appl Mater Interfaces. 2013;5(21):10559–64. doi: 10.1021/am4022973.
[37] Huang S, Yang L, Liu M, Phua SL, Yee WA, Liu W, et al. Complexes of polydopamine-modified clay and ferric ions as the framework for pollutant-absorbing supramolecular hydrogels. Langmuir. 2013;29(4):1238–44. doi: 10.1021/la303855t.
[38] Xu Q, Kong Q, Liu Z, Zhang J, Wang X, Liu R, et al. Polydopamine-coated cellulose microfibrillated membrane as high performance lithium-ion battery separator. RSC Adv. 2014;4(16):7845–50. doi: 10.1039/C3RA45879B.
[39] Poletto M, Pistor V, Santana RMC, Zattera AJ. Materials produced from plant biomass: Part II: Evaluation of crystallinity and degradation kinetics of cellulose. Mater Res. 2012;15:421–7. doi: 10.1590/S1516-14392012005000048.
[40] Khalil U, Shakoor MB, Ali S, Rizwan M, Alyemeni MN, Wijaya L. Adsorption-reduction performance of tea waste and rice husk biochars for Cr (VI) elimination from wastewater. J Saudi Chem Soc. 2020;24(11):799–810. doi: 10.1016/j.jscs.2020.07.001.
[41] Prajapati AK, Das S, Mondal MK. Exhaustive studies on toxic Cr (VI) removal mechanism from aqueous solution using activated carbon of Aloe vera waste leaves. J Mol Liq. 2020;307:112956. doi: 10.1016/j.molliq.2020.112956.
[42] Tran HN, Nguyen DT, Le GT, Tomul F, Lima EC, Woo SH, et al. Adsorption mechanism of hexavalent chromium onto layered double hydroxides-based adsorbents: A systematic in-depth review. J Hazard Mater. 2019;373:258–70. doi: 10.1016/j.jhazmat.2019.03.018.
[43] Alsaiari NS, Katubi KM, Alzahrani FM, Amari A, Osman H, Rebah FB, et al. Synthesis, characterization and application of polypyrrole functionalized nanocellulose for the removal of Cr (VI) from aqueous solution. Polymers. 2021;13(21):3691. doi: 10.3390/polym13213691.
[44] Fan S, Wang Y, Li Y, Tang J, Wang Z, Tang J, et al. Facile synthesis of tea waste/Fe_3O_4 nanoparticle composite for hexavalent chromium removal from aqueous solution. RSC Adv. 2017;7(13):7576–90. doi: 10.1039/C6RA27781K.
[45] Liu C, Jin R-N, Ouyang X-k, Wang Y-G. Adsorption behavior of carboxylated cellulose nanocrystal–polyethyleneimine composite for removal of Cr (VI) ions. Appl Surf Sci. 2017;408:77–87. doi: 10.1016/j.apsusc.2017.02.265.
[46] Zhang K, Li H, Xu X, Yu H. Synthesis of reduced graphene oxide/NiO nanocomposites for the removal of Cr (VI) from aqueous water by adsorption. Microporous Mesoporous Mater. 2018;255:7–14. doi: 10.1016/j.micromeso.2017.07.037.
[47] Ahmadi A, Foroutan R, Esmaeili H, Tamjidi S. The role of bentonite clay and bentonite clay@ $MnFe_2O_4$ composite and their physico-chemical properties on the removal of Cr (III) and Cr (VI) from aqueous media. Environ Sci Pollut Res. 2020;27:1–14. doi: 10.1007/s11356-020-07756-x.
[48] Ho Y-S, McKay G. Kinetic models for the sorption of dye from aqueous solution by wood. Process Saf Environ Prot. 1998;76(2):183–91. doi: 10.1205/095758298529326.
[49] Eltaweil AS, El-Monaem EMA, Mohy-Eldin MS, Omer AM. Fabrication of attapulgite/magnetic aminated chitosan composite as efficient and reusable adsorbent for Cr (VI) ions. Sci Rep. 2021;11(1):1–15. doi: 10.1038/s41598-021-96145-6.
[50] Wang X, Liu X, Xiao C, Zhao H, Zhang M, Zheng N, et al. Triethylenetetramine-modified hollow Fe_3O_4/SiO_2/chitosan magnetic nanocomposites for removal of Cr (VI) ions with high adsorption capacity and rapid rate. Microporous Mesoporous Mater. 2020;297:110041. doi: 10.1016/j.micromeso.2020.110041.
[51] Sadeghi MM, Rad AS, Ardjmand M, Mirabi A. Functionalization of SBA-15 by dithiooxamide towards removal of Co (II) ions from real samples: Isotherm, thermodynamic and kinetic

studies. Adv Powder Technol. 2019;30(9):1823–34. doi: 10.1016/j.apt.2019.05.028.
[52] Alzahrani FM, Alsaiari NS, Katubi KM, Amari A, Elkhaleefa AM, Rebah FB, et al. Magnetic nitrogen-doped porous carbon nanocomposite for Pb (II) adsorption from aqueous solution. Molecules. 2021;26(16):4809. doi: 10.3390/molecules26164809.
[53] Mohammadi H, Ghaedi M, Fazeli M, Sabzehmeidani MM. Removal of hexavalent chromium ions and Acid Red 18 by superparamagnetic $CoFe_2O_4$/polyaniline nanocomposites under external ultrasonic fields. Microporous Mesoporous Mater. 2021;324:111275. doi: 10.1016/j.micromeso.2021.111275.
[54] Alsaiari NS, Amari A, Katubi KM, Alzahrani FM, Harharah HN, Rebah FB, et al. The biocatalytic degradation of organic dyes using laccase immobilized magnetic nanoparticles. Appl Sci. 2021;11(17):8216. doi: 10.3390/app11178216.
[55] Alsaiari NS, Amari A, Katubi KM, Alzahrani FM, Rebah FB, Tahoon MA. The synthesis of magnetic nitrogen-doped graphene oxide nanocomposite for the removal of reactive orange 12 dye. Adsorpt Sci Technol. 2022;2022:9417542. doi: 10.1155/2022/9417542.
[56] Alzahrani FM, Alsaiari NS, Katubi KM, Amari A, Tahoon MA. Synthesis, characterization, and application of magnetized lanthanum (III)-based metal-organic framework for the organic dye removal from water. Adsorpt Sci Technol. 2022;2022:3513829. doi: 10.1155/2022/3513829.
[57] Xu Q, Wang Y, Jin L, Wang Y, Qin M. Adsorption of Cu (II), Pb (II) and Cr (VI) from aqueous solutions using black wattle tannin-immobilized nanocellulose. J Hazard Mater. 2017;339:91–9. doi: 10.1016/j.jhazmat.2017.06.005.
[58] Hu H, Liu J, Xu Z, Zhang L, Cheng B, Ho W. Hierarchical porous Ni/Co-LDH hollow dodecahedron with excellent adsorption property for Congo red and Cr (VI) ions. Appl Surf Sci. 2019;478:981–90. doi: 10.1016/j.apsusc.2019.02.008.
[59] Bhaumik M, Maity A, Srinivasu V, Onyango MS. Enhanced removal of Cr (VI) from aqueous solution using polypyrrole/Fe_3O_4 magnetic nanocomposite. J Hazard Mater. 2011;190(1–3):381–90. doi: 10.1016/j.jhazmat.2011.03.062.
[60] Sobhanardakani S, Jafari A, Zandipak R, Meidanchi A. Removal of heavy metal (Hg (II) and Cr (VI)) ions from aqueous solutions using Fe_2O_3@ SiO_2 thin films as a novel adsorbent. Process Saf Environ Prot. 2018;120:348–57. doi: 10.1016/j.psep.2018.10.002.
[61] Santhosh C, Daneshvar E, Kollu P, Peräniemi S, Grace AN, Bhatnagar A. Magnetic SiO_2@$CoFe_2O_4$ nanoparticles decorated on graphene oxide as efficient adsorbents for the removal of anionic pollutants from water. Chem Eng J. 2017;322:472–87. doi: 10.1016/j.cej.2017.03.144.
[62] Karthik R, Meenakshi S. Removal of Cr (VI) ions by adsorption onto sodium alginate-polyaniline nanofibers. Int J Biol Macromol. 2015;72:711–7. doi: 10.1016/j.ijbiomac.2014.09.023.
[63] Li L, Li Y, Cao L, Yang C. Enhanced chromium (VI) adsorption using nanosized chitosan fibers tailored by electrospinning. Carbohydr Polym. 2015;125:206–13. doi: 10.1016/j.carbpol.2015.02.037.
[64] Avila M, Burks T, Akhtar F, Göthelid M, Lansåker PC, Toprak MS, et al. Surface functionalized nanofibers for the removal of chromium (VI) from aqueous solutions. Chem Eng J. 2014;245:201–9. doi: 10.1016/j.cej.2014.02.034.
[65] Liu F, Wang A, Xiang M, Hu Q, Hu B. Effective adsorption and immobilization of Cr (VI) and U (VI) from aqueous solution by magnetic amine-functionalized SBA-15. Sep Purif Technol. 2021;282:120042. doi: 10.1016/j.seppur.2021.120042.
[66] Liang C, Fu F, Tang B. Mn-incorporated ferrihydrite for Cr (VI) immobilization: Adsorption behavior and the fate of Cr (VI) during aging. J Hazard Mater. 2021;417:126073. doi: 10.1016/j.jhazmat.2021.126073.
[67] Alsaiari NS, Amari A, Katubi KM, Alzahrani FM, Rebah FB, Tahoon MA. Innovative magnetite based polymeric nanocomposite for simultaneous removal of methyl orange and hexavalent chromium from water. Processes. 2021;9(4):576. doi: 10.3390/pr9040576.